

Solar supergranulation revealed by granule tracking

Michel Rieutord, Nadège Meunier*, Sylvain Rondi and Thierry Roudier

Laboratoire d'Astrophysique de Toulouse et Tarbes, UMR 5572, CNRS et Université Paul Sabatier Toulouse 3, 14 avenue E. Belin, 31400 Toulouse, France

e-mail: rieutord@ast.obs-mip.fr, nmeunier@obs.ujf-grenoble.fr, rondi@wanadoo.fr, roudier@ast.obs-mip.fr

November 2, 2007

ABSTRACT

Context. Supergranulation is a pattern of the velocity field at the surface of the Sun which has been known for more than fifty years. However, no satisfactory explanation of its origin has been proposed yet.

Aims. New observational constraints are therefore needed to guide theoretical approaches which hesitate between scenarii which either invoke a large-scale instability of turbulent convection or a direct forcing by buoyancy.

Methods. Using a 7.5 h-long sequence of high resolution images of unprecedented size, together with tracking granules, we have determined the velocity field at the Sun's surface in great details from a scale of 2.5 Mm up to a scale of 250 Mm.

Results. The kinetic energy density spectrum shows that supergranulation peaks at 36 Mm and spans on scales ranging between 20 Mm and 75 Mm. The decrease of supergranular flows in the small scales is close to a k^{-2} -powerlaw, steeper than the equipartition Kolmogorov one. The probability distribution functions of the divergence field shows the signature of intermittency of the supergranulation and thus its turbulent nature.

Key words. Hydrodynamics – Sun: convection

1. Introduction

Supergranulation has been discovered by Hart (1954) using Doppler images of the Sun. It appeared as an essentially horizontal flow field at a typical scale of 30 Mm. The origin of this flow field was first thought to be related to the second ionization of helium which provides some latent heat at a depth around 10 Mm compatible with their typical size (Simon & Weiss, 1968). This scenario has been much debated because of the weakness of the effect and the apparent vigour of the supergranular flow. Other ways of generating this velocity scale rely on large-scale instabilities of the surface turbulent flow (Rieutord et al., 2000), triggered by the strong density stratification which easily transforms vertical motion into horizontal one thanks to mass conservation. In this scenario, kinetic energy of granules, the small-scale convective cells, is thought to be piped to larger scale by an AKA-like effect (Gama et al., 1994). However, still other kind of large-scale instabilities are possible like a convective instability triggered by fixed flux boundary conditions imposed by the small-scale granular convection (Rincon & Rieutord, 2003). In this approach, the cooling resulting from the granulation does not suppress the convective instability of the larger scales; because all the heat flux is carried by the small

scale, none is carried by the large scale instability which shows up without (or little) temperature fluctuations.

Obviously, supergranulation theory needs guidance from every available observational constraint. This letter presents the results of the observations issued from the CALAS project (a CAmera for the LARge scales of the Sun) collecting a sequence of high resolution wide field images which have allowed us to capture the evolution of a hundred of supergranules at disk center during 7.5h. We can thus give new constraints on the dynamics of the solar surface in the supergranulation range. After a brief description of the data set (Sect. 2), we show the spectral side of the supergranular flow (Sect. 3) as well as the probability distribution functions of the divergences (Sect. 4); first conclusions follow.

2. Observational technics and data reduction

2.1. Data set

On 13 march 2007, we observed the Sun at disc centre during 7.5 h using the Lunette Jean Rösch at Pic du Midi, a 50 cm-refractor. Images were taken at $\lambda = 575 \pm 5\text{nm}$, with a 14Mpixel CMOS-camera (4560×3048), with 0.115 arcsec/pixel, thus covering of $524 \times 350 \text{ arcsec}^2$ (see Fig. 1). 10811 images have been obtained with a regular cadence of one every 2.5s. Then, two independent series of ~ 1400 images have been extracted.

Send offprint requests to: M. Rieutord

* Present address: Laboratoire d'Astrophysique, Observatoire de Grenoble, BP 53, 38041 Grenoble cedex 9

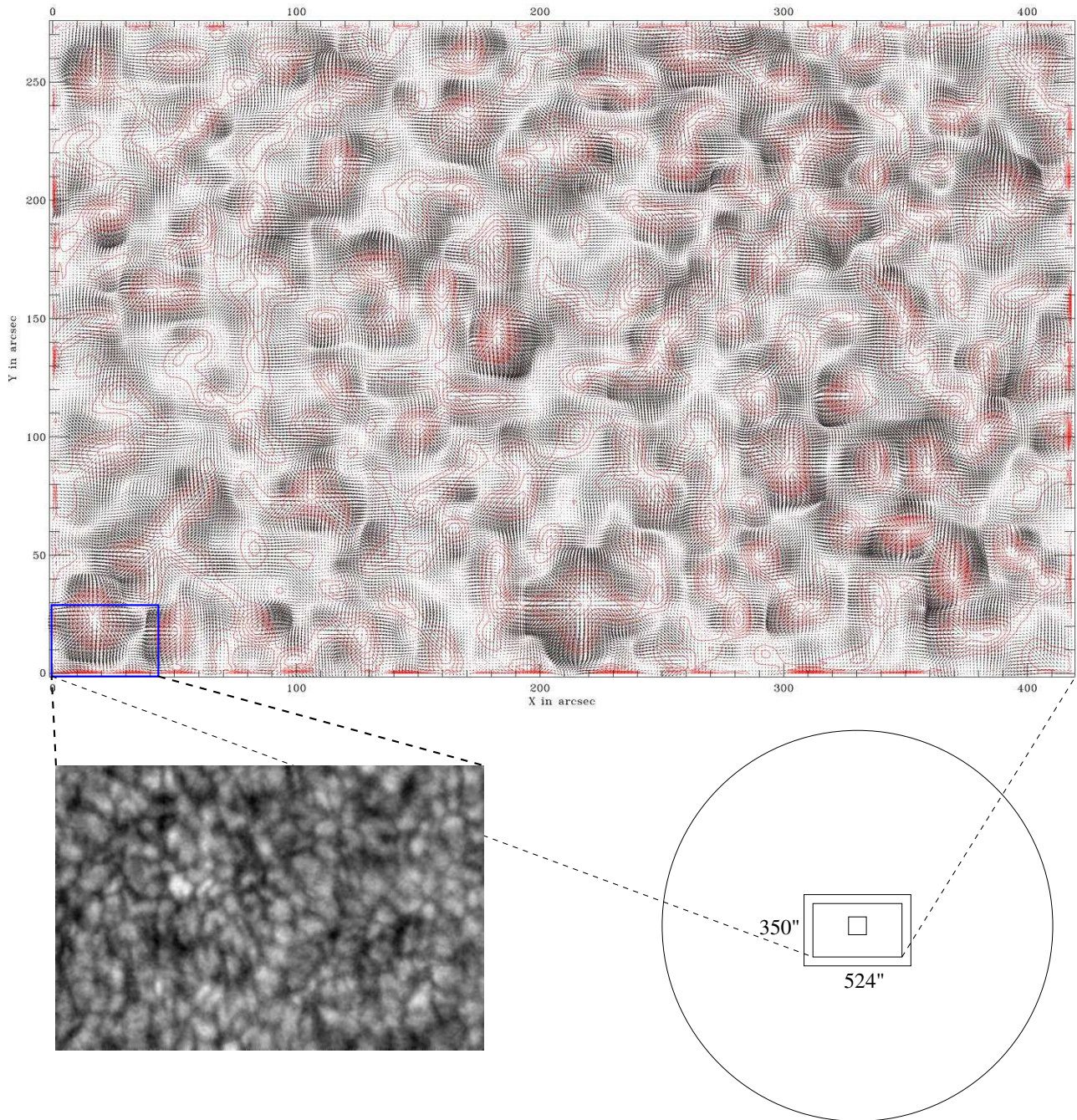


Fig. 1. Low right: The CALAS field of view on the Sun: the large rectangle indicates the size of images, the smaller one shows the field where the velocities could be computed, while the small square shows the field of view of the SOT instrument on the Hinode satellite when tracking granules. Top: the supergranulation velocity field with the divergence contours superimposed (scales shorter than 8 Mm have been filtered out). A time-window of 150 min has been used. Low left: a zoom on granulation showing the relative sizes of granules and supergranules.

They sample the same solar signal with a period of 20s but are noised differently by the Earth atmospheric perturbations. The comparison between the outputs of both series allows us to evaluate the influence of the seeing and test the robustness of the results with respect to this noise.

Because of tracking constraints, the common field of each series reduced to $\sim 400 \times 300$ arcsec², thus covering a surface of 290×216 Mm² on the Sun (Fig. 1).

After recentering, images have been $k - \omega$ filtered so as to remove as much as possible, Earth atmospheric distortion

which is the main source of noise for velocity measurements (Tkaczuk et al., 2007).

2.2. Velocity fields

Horizontal velocity fields have been obtained using the CST granule tracking algorithm (Roudier et al., 1999, Rieutord et al., 2007). As shown in Rieutord et al. (2001) granules motions trace large-scale velocity fields when the scale is larger than 2.5 Mm. Hence, we sampled the velocity field with a bin of 12 pixels (~ 1 Mm).

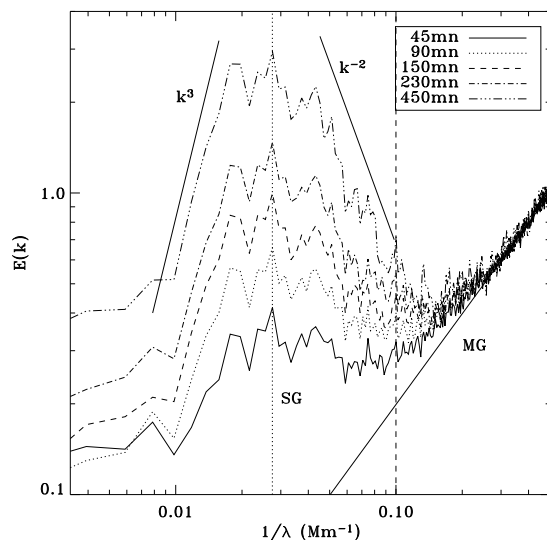


Fig. 2. Kinetic energy spectra obtained for various time windows. The vertical dotted line indicates the position of the peak at 36.4 Mm. The vertical dashed line emphasizes the 10 Mm scale, usually taken as the upper limit of mesogranular scale. Two power laws are shown on each side of the peak to give an idea of the slopes.

The velocities are obtained with the tracking of granules during a given time window. Thus we have access to average velocity components, namely $\overline{v}_x(i, j)$ and $\overline{v}_y(i, j)$, where the overline refers to the time averaging imposed by the time window. This averaging improves the signal-to-noise ratio, but naturally decreases the time resolution. Typically, the shortest time window that could be used is 30 min long.

Although the field is large, projection effects of the spherical Sun are still of weak influence. At most, in the field corners, the correction on the velocity would be less than 4%, which is much less than the noise.

We show in Fig. 1 an example of these velocity fields. The small-scale components of the flow (with scales below 8 Mm) have been filtered out using Daubechies wavelets. (see Rieutord et al., 2007). Figure 1 shows that robust steady supergranules live among a wide variety of flow structures illustrating the turbulent nature of these scales and their wide spectral range.

3. The kinetic energy spectrum

A convenient way to view the dynamics of a flow is to examine the spectral content of the velocity field. We thus computed the spectral density of kinetic energy $E(k)$ associated with the horizontal flow that we can measure. It is such that

$$\frac{1}{2} \langle \overline{v}^2 \rangle = \int_0^\infty E(k) dk$$

$E(k)$ is displayed in Fig. 2 for the flows determined with various time-windows. The short time-windows of 45 min give us 10 independent spectra which are averaged together, while the whole series 450 mn time-window gives us only one spectrum. Note that no spatial filtering was applied to the velocity field. We clearly see that $E(k) \propto k$ at small scale, which is the signature of decorrelated random noise.

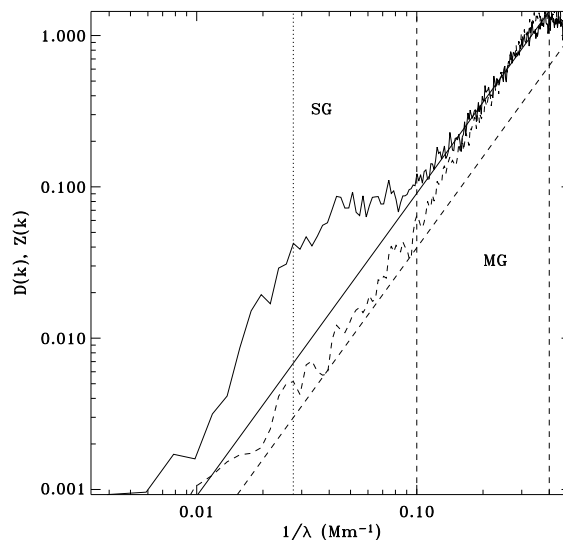


Fig. 3. Same as in Fig. 2 but for the horizontal divergence of the flow, $\partial_x v_x + \partial_y v_y$ (solid line) and for the vertical vorticity, $\partial_x v_y - \partial_y v_x$ (dashed line); the supergranulation peak is clearly visible at $\lambda = 36$ Mm in the divergence spectrum but absent in the vorticity one.

These spectra clearly show the emergence of the spectral range of the supergranulation as the length of the time-window increases. Let us point out the remarkable stability of the wavenumber of the spectral peak when the time averaging is changed. This demonstrate (if necessary!) that supergranulation is a genuine velocity field at the Sun's surface. It is not the consequence of time-averaging the small, fast turning-over small scales. Of course, if the averaging interval is long enough (i.e. of the order of the turn-over time scale of supergranulation), the spectral peak will move to ever larger scales before disappearing. The present spectra peak at a wavelength of 36 Mm. The FWHM of the peak indicates that supergranulation occupies the range of scales of [20, 75] Mm.

The present mean value of the diameter of supergranules broadly agrees with the previous determinations. However, our value is slightly higher than some recent measurement. For instance, Meunier et al. (2007) find a mean diameter of 31.4 Mm with a technique based on the segmentation of the divergence field derived from velocities issued from a local correlation technique applied to SOHO/MDI white light images. Del Moro et al. (2004) use also a divergence field but derived from time-distance helioseismology; they find a mean size of 27 Mm, significantly smaller than ours.

The difference may, most likely, come from the technique of measurement although we cannot exclude some influence of the solar cycle as our data have been taken on a Sun showing no activity. As far as the method is concerned, let us emphasise that ours is certainly the most direct; the use of divergence, which is a derivative of the velocity field, is always delicate and more sensitive to noise than the original velocity.

In Fig. 2 we also indicate the best-fit power laws which mimic the sides of the supergranulation peak. We find that $E(k) \sim k^3$ on the large-scale side and $E(k) \sim k^{-2}$ on the

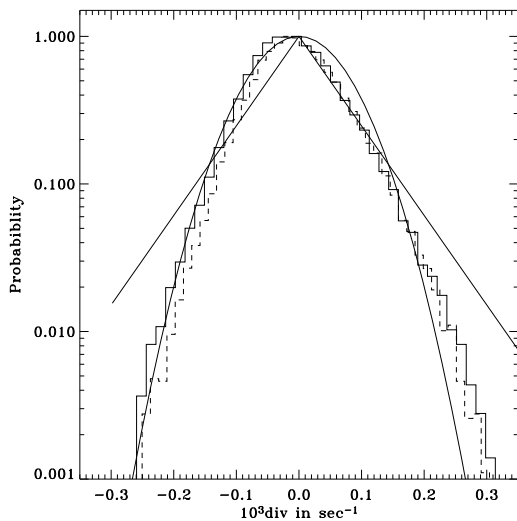


Fig. 4. Histograms of the divergences; solid and dashed lines have the same solar signal but a different noise from Earth atmosphere. Scales below 8 Mm have been filtered out. A gaussian and an exponential distributions are overplotted for comparison.

small-scale one. This latter power law is steeper than the $-5/3$ Kolmogorov one and may be an effect of density stratification.

To complete the spectral picture, we also show, in Fig. 3 the spectra of the horizontal divergence of the velocity field and of the vertical vorticity. Beyond the k^2 -dependence of the spectral densities, which is a consequence of the derivative of uncorrelated noise, we can see that the divergence spectrum clearly shows the supergranulation peak while the vertical vorticity shows no signal in this range. The vorticity does show some weak signal however, but in the mesogranulation range, below 10 Mm.

4. Probability density functions

Another way to look at the velocity fields is to consider the probability density functions. Such distributions have been computed for the velocity field, its divergence and its curl. We show in Fig. 4 the distribution of the divergence field when scales shorter than 8 Mm have been filtered out of the velocity field. This distribution clearly shows larger wings than the gaussian one with identical width. We also note that the noise of Earth atmosphere is weak enough, and does not perturb the result. This trend to an exponential distribution is a signature of intermittency (e.g. Rieutord, 1997). Such a result was also observed by Meunier et al. (2007) with a completely different set of data and method. Thus, the intermittency of supergranulation seems to be a robust property. Exponential wings are usually less visible on the velocity (e.g. Vincent & Meneguzzi, 1991), and indeed are barely noticeable in our data. As far as vorticity is concerned, the noise is unfortunately too high to give convincing measurements.

5. Conclusions

For the first time, it has been possible to follow the motion of well-resolved granules in a large field of view. The spectral peak of supergranulation has thus been determined with pre-

cision. According to our data, supergranulation has the most energetic motions at a scale of 36 Mm and encompass all the scales ranging from 20 to 75 Mm as shown by the FWHM of the peak. Except its amplitude, this peak is not sensitive to the time window used to measure the granules motions. The signal also clearly appears in the divergence spectral density, but not in the vorticity; likely, vorticity at supergranulation scale near the Sun's equator is much weaker and does not emerge from the noise.

Finally, our data confirm the fact that supergranulation has a noticeable degree of intermittency, clearly appearing in the distribution of divergence values.

As far as the origin of supergranulation is concerned, the scenarii mentioned in the introduction can be tested with these data, either in the real space with velocity fields like the one shown in Fig. 1 or in the spectral space with the given spectra.

Further work on the observational side will focus on the determination of the third component of the velocity field, the increase of the field size and the reduction of the noise, so as to further constrain the dynamics of scales from the granulation one to the 100 Mm one.

Acknowledgements. The CALAS project has been financially supported by the French ministry of education (ACI), by the Programme National Soleil-Terre of CNRS and the Observatoire Midi-Pyrénées. We are also very grateful to the “Groupe d’Instrumentation des Grands Télescopes (GIGT)” of the laboratory, for their technical help at various phase of the project, especially to Francis Beigbeder, Elodie Bourrec and Laurent Parès. We also wish to thank René Dornic for his efficient support in mechanical realizations and Philippe Saby for his help in sorting out the right computing hardware. SR wishes to thank the CNRS for its support during his PhD thesis which much contributed to the project.

References

- Del Moro, D., Berilli, F., Duvall, T., & Kosovichev, A. 2004, *Solar Phys.*, 221, 23
- Gama, S., Vergassola, M., & Frisch, U. 1994, *J. Fluid Mech.*, 260, 95
- Hart, A. B. 1954, *MNRAS*, 114, 17
- Meunier, N., Tkaczuk, R., Roudier, T., & Rieutord, M. 2007, *A&A*, 461, 1141
- Rieutord, M. 1997, *Une introduction à la dynamique des fluides (Masson)*
- Rieutord, M., Roudier, T., Ludwig, H.-G., Nordlund, Å., & Stein, R. 2001, *A & A*, 377, L14
- Rieutord, M., Roudier, T., Malherbe, J. M., & Rincon, F. 2000, *A & A*, 357, 1063
- Rieutord, M., Roudier, T., Roques, S., & Ducottet, C. 2007, *A & A*, 471, 687
- Rincon, F. & Rieutord, M. 2003, in *SF2A-2003: Semaine de l’Astrophysique Française*, ed. F. Combes, D. Barret, T. Contini, & L. Paganì, 103–+
- Roudier, T., Rieutord, M., Malherbe, J., & Vigneau, J. 1999, *A & A*, 349, 301
- Simon, G. W. & Weiss, N. O. 1968, *Zeit. für Astrophys.*, 69, 435
- Tkaczuk, R., Rieutord, M., Meunier, N., & Roudier, T. 2007, *A & A*, 471, 695
- Vincent, A. & Meneguzzi, M. 1991, *J. Fluid Mech.*, 225, 1